Mon. Not. R. Astron. Soc. **000**, 1–6 (2015) Printed 13 February 2015 (MN LATEX style file v2.2)

The Initial Mass Function of Early-type Galaxies: no correlation with [Mg/Fe]

Francesco La Barbera[1⋆], Ignacio Ferreras[2], Alexandre Vazdekis[3,4]
[1] *INAF-Osservatorio Astronomico di Capodimonte, sal. Moiariello 16, Napoli, 80131, Italy*
[2] *Mullard Space Science Laboratory, University College London, Holmbury St Mary, Dorking, Surrey RH5 6NT, UK*
[3] *Instituto de Astrofísica de Canarias, Calle Vía Láctea s/n, E-38205 La Laguna, Tenerife, Spain*
[4] *Departamento de Astrofísica, Universidad de La Laguna (ULL), E-38206 La Laguna, Tenerife, Spain*

arXiv:1502.03449v1 [astro-ph.GA] 11 Feb 2015

MNRAS Letters, Revised version 13 February 2015

ABSTRACT
The Initial Mass Function (IMF) of early-type galaxies (ETGs) has been found to feature systematic variations by both dynamical and spectroscopic studies. In particular, spectral line strengths, based on gravity-sensitive features, suggest an excess of low-mass stars in massive ETGs, i.e. a bottom-heavy IMF. The physical drivers of IMF variations are currently unknown. The abundance ratio of α elements, such as [Mg/Fe], has been suggested as a possible driver of the IMF changes, although dynamical constraints do not support this claim. In this letter, we take advantage of the large SDSS database. Our sample comprises 24,781 high-quality spectra, covering a large range in velocity dispersion ($100<\sigma_0<320$ km s^{-1}) and abundance ratio ($-0.1<$[Mg/Fe]$<+0.4$). The large volume of data allows us to stack the spectra at fixed values of σ_0 and [Mg/Fe]. Our analysis – based on gravity-sensitive line strengths – gives a strong correlation with central velocity dispersion and a negligible variation with [Mg/Fe] at fixed σ_0. This result is robust against individual elemental abundance variations, and seems not to raise any apparent inconsistency with the alternative method based on galaxy dynamics.

Key words: galaxies: stellar content – galaxies: fundamental parameters – galaxies: formation

1 INTRODUCTION

The stellar IMF, i.e. the mass distribution of stars in a stellar population (hereafter SP) at birth, has been largely assumed to be universal, mostly because of lack of evidence regarding variations of the IMF among star clusters and OB associations in our Galaxy (e.g. Chabrier 2003; Kroupa et al. 2010). However, recent studies, based on independent techniques, such as dynamics (e.g. Cappellari et al. 2012; Dutton et al. 2013; Tortora et al. 2013), lensing (e.g. Auger et al. 2010; but see Smith & Lucey 2013), and spectroscopy (e.g. Cenarro et al. 2003; van Dokkum & Conroy 2010; Spiniello et al. 2014; as well as Ferreras et al. 2013; La Barbera et al. 2013, hereafter F13 and LB13, respectively), have found that the IMF varies systematically with galaxy mass in ETGs.

The origin of this systematic variation remains unknown. Conroy & van Dokkum (2012b, hereafter CvD12b) found, for a sample of 38 nearby ETGs, that the IMF normalization (i.e. the stellar M/L, normalized with respect to a MW-like IMF) correlates more strongly with the abundance of α-elements, such as [Mg/Fe], than with central velocity dispersion (σ_0), claiming that [Mg/Fe], which is a proxy for the star-formation time-scale (Thomas et al. 2005; de la Rosa et al. 2011), might be the main driver of the IMF in ETGs. However, this finding is challenged by the fact that dynamical constraints, for a subsample of 34 ETGs in common between CvD12b and ATLAS^{3D} (Cappellari et al. 2013), correlate better with σ_0 than [Mg/Fe] (Smith 2014). Furthermore, no correlation of dynamical constraints with SP parameters has been detected in the ATLAS^{3D} sample (McDermid et al. 2014). Given the importance of constructing a comprehensive theory of a non-universal IMF (e.g. Hopkins 2013; Chabrier, Hennebelle, Charlot 2014; Ferreras et al. 2015), the above inconsistencies call for further investigations, based on larger samples, of the possible drivers of IMF variations. In LB13, we assembled a battery of 126 stacked spectra, with varying σ_0 and [Mg/Fe], finding that gravity-sensitive features in ETGs depend very mildly on [Mg/Fe] at fixed σ_0. Such a result suggests no correlation between IMF and [Mg/Fe]. In the present letter, we comple-

⋆ E-mail: labarber@na.astro.it

© 2015 RAS

ment the results of LB13, performing a *quantitative* analysis of how the IMF slope depends on both σ_0 and [Mg/Fe].

2 DATA

The SPIDER sample (La Barbera et al. 2010a, hereafter LB10) consists of 39,993 nearby ($0.05 < z < 0.095$) ETGs, selected from Data Release 6 of the Sloan Digital Sky Survey (SDSS, Adelman-McCarthy et al. 2008). ETGs are defined as bulge-dominated systems, featuring passive spectra within the SDSS fibres. All SPIDER ETGs have SDSS spectra available, covering the spectral range from 3800 to 9200 Å, with a spectral resolution $\sigma_{inst} \sim 60\,\mathrm{km\,s^{-1}}$. For each spectrum, we use its central velocity dispersion, σ_0, from the SDSS database, and an empirical proxy, [Z_{Mg}/Z_{Fe}], for the [Mg/Fe] abundance ratio (see LB13 for details). The [Z_{Mg}/Z_{Fe}] is the difference of total metallicity estimates, [Z/H], measured from the Mgb5177 and Fe3= (Fe4383 + Fe5270 + Fe5335)/3 spectral indices, respectively. Total metallicities are measured at fixed age (estimated with the spectral fitting code STARLIGHT; Cid Fernandes et al. 2005), comparing observed line strengths to predictions of MILES Simple Stellar Population (SSP) models (Vazdekis et al. 2012). As shown in LB13, [Z_{Mg}/Z_{Fe}] is tightly correlated with [α/Fe], derived from SP models taking abundance ratios into account (Thomas, Maraston & Johansson 2011), with [α/Fe] ~ 0.55 [Z_{Mg}/Z_{Fe}]. Since Mg is the reference α-element of an SP model, and both Mgb5177 and Fe3 are mostly sensitive to the abundance of Mg and Fe, respectively (see, e.g., Johansson et al. 2012, hereafter JTM12), in this letter we use [Mg/Fe] rather than [α/Fe], with the conversion [Mg/Fe]~ 0.55[Z_{Mg}/Z_{Fe}]. Notice that since [Z_{Mg}/Z_{Fe}] actually measures [Mg/Fe], our conclusions do not rely on the assumption that α elements should track each other (see, e.g., Kuntschner et al. 2010). Following LB13 and F13, we restrict the analysis to a subsample of 24,781 SPIDER ETGs, with (i) $100 \leqslant \sigma_0 \leqslant 320\,\mathrm{km\,s^{-1}}$, (ii) low internal extinction (i.e. a color excess estimate $E(B-V) < 0.1$), and (iii) better signal-to-noise (S/N) ratio (see below). We classify the spectra into 18 narrow bins of σ_0(see LB13 for details), each bin with a width of $10\,\mathrm{km\,s^{-1}}$, except for the last two, for which we adopt the range [260, 280], and [280, 320] $\mathrm{km\,s^{-1}}$, respectively. For each bin, we only select spectra whose S/N ratio is higher than the lowest quartile of the S/N distribution in that bin.

In the present letter, we analyze the median-stacked spectra assembled by LB13 for this sample, i.e. (i) the 18 "σ_0 stacks", obtained by selecting all ETGs in each σ_0 bin, and (ii) the "[Z_{Mg}/Z_{Fe}] sub-stacks", assembled by selecting, for each bin in σ_0, those ETGs (1) below the 10-th, (2) below the 25-th, (3) between the 25-th and 50-th, (4) between the 50-th and 75-th, (5) above the 75-th, and (6) above the 90-th percentiles of the [Z_{Mg}/Z_{Fe}] distribution. This procedure yields 18 σ_0 stacks, plus $18 \times 6 = 108$ [Z_{Mg}/Z_{Fe}] sub-stacks, for a total of 126 stacked spectra. At fixed σ_0, the [Z_{Mg}/Z_{Fe}] stacks span a range of $\delta([Z_{Mg}/Z_{Fe}]) \sim 0.6$ (corresponding to δ([Mg/Fe]) ~ 0.3), allowing us to single out the effect of σ_0 and abundance ratio on IMF slope.

3 ANALYSIS

We rely on the extended MILES (MIUSCAT) SP models (Vazdekis et al. 2012) with age (total metallicity) $4 < t < 14\,\mathrm{Gyr}$ ($-0.4 <$[Z/H]$< +0.22$), and ten choices of a bimodal IMF (Vazdekis et al. 1996), i.e. a power-law, with slope Γ_b in log-mass units, smoothly tapered to a constant value towards low-mass stars ($\lesssim 0.6 M_\odot$), with $0.3 \leqslant \Gamma_b \leqslant 3.3$. Note that $\Gamma_b \sim 1.3$ gives a good representation of a Kroupa (MW-like) distribution, while higher values of Γ_b correspond to bottom-heavier distributions. For each stacked spectrum, we derive Γ_b by a similar procedure to LB13 (see also F13 and Martín-Navarro et al. 2015, hereafter MN15). We minimize the expression:

$$\chi^2(t,[\mathrm{Z/H}],\Gamma_b,[X/\mathrm{Fe}]) = \sum_i \left[\frac{E_i - E_{M,i} - \sum_X \Delta_{i,X}\cdot[X/\mathrm{Fe}]}{\sigma_i}\right]^2, \quad (1)$$

where E_i and $E_{M,i}$ are observed and model line-strengths for a selected set of spectral features, [X/Fe] is the abundance ratio of different chemical elements (see below), $\Delta_{i,X}$ is the sensitivity of the i-th line strength to a given elemental abundance, i.e. $\Delta_{i,X} = \delta(E_{M,i})/\delta([X/\mathrm{Fe}])$, and σ_i is the uncertainty on E_i, obtained by adding in quadrature the statistical error on E_i with its *intrinsic* uncertainty (see sec. 6 of LB13). The $E_{M,i}$ are computed with MIUSCAT models, while the $\Delta_{i,X}$ factors use the publicly available Conroy & van Dokkum (2012a, hereafter CvD12a) stellar population models, having solar metallicity, old age ($t = 13.5\,\mathrm{Gyr}$), and a Kroupa IMF. The free fitting parameters in Eq. 1 are age, metallicity, IMF slope, and elemental abundances. Both $E_{M,i}$ and $\Delta_{i,X}$ are computed by matching the spectral resolution of the models to that of each stacked spectrum. Errors on best-fitting parameters are computed with a bootstrap approach, shifting observed line-strengths according to their uncertainties. Notice that by varying the Γ_b, we actually alter the relative fraction of low- to high-mass stars in the IMF by changing the behaviour at higher masses ($\gtrsim 0.6 M_\odot$). Although this is different from changes in a unimodal (single power-law) distribution (e.g. CvD12a), in practice, gravity-sensitive features are only sensitive to the mass fraction of low-mass stars in the IMF (see figure 19 of LB13).

To test how abundance ratios may affect the estimate of Γ_b, we adopt two alternative methods, differing for the selected set of spectral features and elemental abundances included in the fitting (see Tab. 1):

1SSP (Single Burst) method - We use the same set of spectral features as in LB13, except for the Calcium triplet, CaT, which cannot be measured over the SDSS spectral range for most SPIDER ETGs, and is replaced by the Ca2 feature alone (see MN15). No [X/Fe] term is included in the fits. Indeed, we found that, overall, the leading abundance ratios of gravity-sensitive features have a negligible impact on relative variations of Γ_b (see, e.g., green and cyan curves in figure 12 of LB13). In contrast to our previous works, we do not apply any [Mg/Fe] empirical correction to bring observed line-strengths to solar-scale, as (i) the variation of most gravity sensitive-features with σ_0 is much stronger than that with [Mg/Fe] (LB13), and (ii) our aim, in the present letter, is to constrain the IMF as a function of both σ_0 and [Mg/Fe], hence we do not want to apply, *a priory*, any [Mg/Fe] correction.

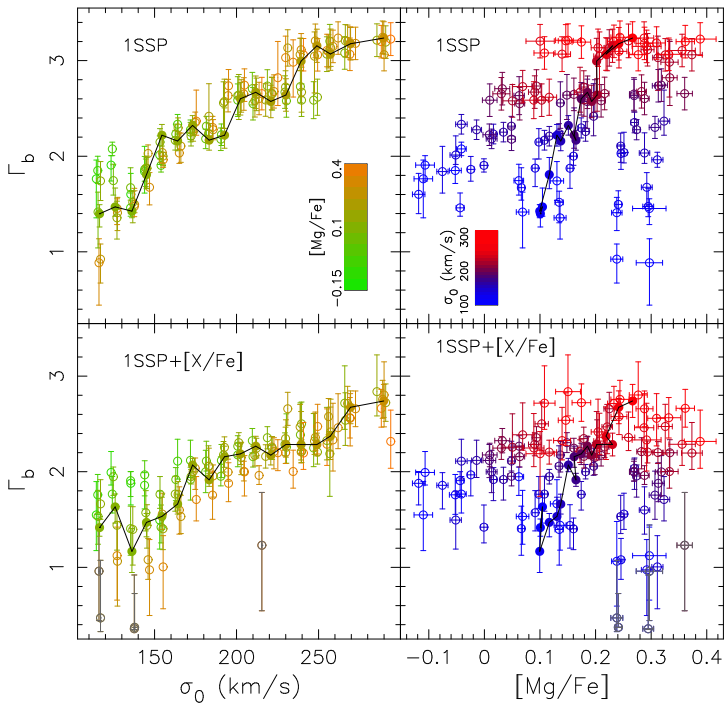

Figure 1. Trends of Γ_b with σ_0 (left-) and [Mg/Fe](right-panels) for our 126 SDSS-based stacked spectra. Upper and lower panels correspond to the 1SSP and 1SSP+[X/Fe] fitting methods to infer the IMF slope (see Sec. 3). The σ_0 stacks (see Sec. 2) are plotted with filled circles, and connected by a black curve, while the sub-stacks with varying [Mg/Fe] are plotted with empty circles. Error bars are quoted at the $1\,\sigma$ confidence level. Blue-through-red colors (*right*) encode, as in LB13, the increase of σ_0; whereas green-through-orange (*left*) correspond to the range in [Mg/Fe]. Stacks with a large uncertainty ($> 50\%$) on Γ_b are plotted in grey (bottom-panels; see the text). Notice the tight (poor) correlation of Γ_b with σ_0 ([Mg/Fe]) for both fitting methods.

1SSP+[X/Fe] *method* - We fit all individual abundance ratios, whose $\Delta_{i,X}$ can be computed with CvD12a models, and adopt a much wider set of Lick-based features than in the 1SSP case, making sure to include, for each [X/Fe], at least one index with prominent sensitivity to it (based on figure 1 of JTM12), as summarized in Tab. 1. Notice that the values of $\Delta_{i,X}$ may not be constant as a function of age (as assumed in Eq. 1), as index responses to abundance variations could become milder towards younger ages with respect to those found in massive ETGs (Sansom et al. 2013), implying that 1SSP models, instead of 1SSP+[X/Fe], might describe better our low-σ stacks (leaving unchanged the conclusions, see below). Moreover, since CvD12a models (i.e. the $\Delta_{i,X}$ factors) work at fixed Fe, rather than total metallicity (MILES), the [Z/H] from Eq. 1 does not necessarily measure the total metallicity. This is nevertheless unimportant for the present letter, as we study trends with $[Z_{Mg}/Z_{Fe}]$, rather than [Z/H] (see Martín-Navarro et al., in preparation) .

We notice that for each stack, the Hβ_o age indicator is corrected for nebular emission, as in LB13.

4 RESULTS

Fig. 1 shows the best-fitting Γ_b, for all stacked spectra, vs. σ_0 (left-) and [Mg/Fe] (right-panels), respectively. The σ_0 ([Mg/Fe]) stacks (see Sec.2) are plotted with filled (empty) circles. Regardless of the fitting method (upper vs. lower panels), and in particular even when taking abundance ratios into account (1SSP+[X/Fe] method), we find a tight correlation between Γ_b and σ_0, consistent with previous spectroscopic studies (e.g. CvD12b, LB13). Notice that the quality of the fits is generally good for all stacks, with a reduced $\chi^2 \sim 2$ (~ 1) for the 1SSP (1SSP+[X/Fe]) methods (see sec. 7 of LB13), and – most importantly for the present work – no significant χ^2 dependence on either σ_0 or [Mg/Fe] is found. The Γ_b-σ_0 relation is shallower for the 1SSP+[X/Fe] case (see below), consistent with the fact that different Γ_b-σ_0 slopes are found when adopting different sets of spectral features (F13, Spiniello et al. 2014), and/or different methodologies (LB13, Spiniello et al. 2015). For the present work, we do not aim to establish which method provides a more reliable Γ_b-σ_0 relation, but, rather, to test the robustness of our results against two rather extreme cases, namely, the 1SSP method, where the impact of abundance ratios is neglected; and the 1SSP+[X/Fe] approach, where we attempt to model the effect of individual elemental abundances, with theoretical (CvD12a) stellar population models (whose ingredients, such as the stellar atmosphere calculations, are nevertheless affected by their own uncertainties).

Fig. 1 shows that, regardless of the methodology, the Γ_b exhibits a far more dispersed correlation with [Mg/Fe] than σ_0, i.e. [Mg/Fe] is not the main driver of the IMF variations in ETGs. The fact that Γ_b tends to marginally increase with [Mg/Fe] mostly stems from the lack of galaxies with low-[Mg/Fe] (< 0.1) at the highest σ_0 (see red symbols in the right panels of Fig. 1) and the fact that [Mg/Fe] increases

Table 1. Methods to derive the IMF slope, Γ_b. Col. 1 labels the method, while cols. 2 and 3 report the selected list of fitted spectral features and elemental abundances ([X/Fe]), respectively. For the 1SSP+[X/Fe] approach, we include the 1SSP features (from LB13), plus other Lick-based abundance-sensitive indices (marked with superscripts in col. 2). For each [X/Fe] in col. 3, we report the superscripts corresponding to the spectral feature(s) with prominent sensitivity to it.

Method (1)	EW (2)	[X/Fe] (3)
1SSP	Hβ_o, [MgFe]$'$, TiO1, TiO2, Mg4780, Na8190$_{SDSS}$, Ca2, CaHK, NaD	none
1SSP+[X/Fe]	Hβ_o, [MgFe]$'$, TiO1, TiO2, Mg4780, Na8190$_{SDSS}$, Ca2, Ca1, Ca4227^1 , NaD^2 , Fe4531^3, Mg1^4, Mg2^5, C4668^6, CN2^7, Mgb5177^8	[Ca/Fe]^1, [Na/Fe]^2, [Ti/Fe]^3, [O/Fe]^{4,7}, [C/Fe]^{6,4} [N/Fe]^7, [Mg/Fe]^{5,8}, [Si/Fe]^{4,5}

Table 2. Best-fitting coefficients, A_1, A_2, and A_3 (cols. 2–4), of Eq. 2, for different methods to derive Γ_b (col. 1). The row labeled "$\cdots$+[Mg/Fe]*" corresponds to results for 1SSP+[X/Fe] fits when replacing [Mg/Fe] in Eq. 2, with [Mg/Fe]* (see the text).

Method (1)	A_1 (2)	A_2 (3)	A_3 (4)
1SSP	3.76 ± 0.16	-0.08 ± 0.40	1.95 ± 0.02
1SSP+[X/Fe]	2.92 ± 0.24	-0.93 ± 0.15	1.60 ± 0.02
$\cdots$ +[Mg/Fe]*	2.80 ± 0.22	-0.90 ± 0.14	1.56 ± 0.02

with σ_0 in ETGs (e.g. Thomas et al. 2005). To illustrate this point, we fit a bivariate relation to the data,

$$\Gamma_b = A_1 \log\sigma_0 + A_2[\mathrm{Mg/Fe}] + A_3. \quad (2)$$

This approach is the same as Smith (2014, hereafter S14), with the noticeable difference that in the present work we study the IMF slope, Γ_b, rather than its overall normalization. Eq. 2 allows us to single out, quantitatively, the contribution of [Mg/Fe] and σ_0 to the systematic variations in the IMF. We derive A_1, A_2, and A_3 (see Tab. 2) with a robust least-square fitting procedure, minimizing absolute residuals to Γ_b, excluding those stacks with large ($> 50\%$) uncertainty on Γ_b (see grey symbols in Fig. 1). Fig. 2 plots the best-fitting slopes, A_1 and A_2, for different fitting methods together with their bootstrapped confidence contours, with red and blue colours corresponding to 1SSP and 1SSP+[X/Fe] results, respectively. The green dot and ellipses represent the 1SSP+[X/Fe] slopes obtained by replacing [Mg/Fe] in Eq. 2 with [Mg/Fe]*, i.e. the best-fitting [Mg/Fe] from 1SSP+[X/Fe] fits. In the 1SSP method, no significant correlation with [Mg/Fe] is found at fixed σ_0, as A_2 is consistent with zero at less than $1\,\sigma$, whereas in the 1SSP+[X/Fe] case, A_2 is significantly negative, i.e. Γ_b tends to *decrease* with [Mg/Fe] at fixed σ_0. Notice that between these two methods, there is a $\sim 20\%$ difference in A_1, with shallower slopes for the 1SSP+[X/Fe] case, consistent with Fig. 1. Furthermore, given the range of $\log\sigma_0$ (~ 1.2 dex) and [Mg/Fe] (~ 0.3 dex) probed by the data, the values of A_1 and A_2 for the 1SSP+[X/Fe] method imply a narrower variation in the IMF slope at fixed velocity dispersion, with respect to the variations associated to σ_0. Hence, both approaches agree on [Mg/Fe] having a minor role in the IMF trend of ETGs.

5 SUMMARY AND DISCUSSION

We have assessed in this letter the relative role of central velocity dispersion and [Mg/Fe] abundance ratio as drivers of the systematic variation found in the IMF of ETGs. We assemble a set of 126 high-quality spectra from a sample of 24,781 nearby ETGs (LB13). We split the range in central velocity dispersion ($100 < \sigma_0 < 320$ km s^{-1}) into 18 bins. For each bin, i.e. at fixed σ_0, we create six stacks according to [Mg/Fe], covering a range Δ[Mg/Fe]~ 0.3 dex. For each of the 126 stacks (i.e. including the original 18 stacks in LB13 only binned with respect to σ_0), we derive the slope of the (bimodal) IMF, Γ_b, assuming a single burst, and considering both a direct fit to the line strengths (1SSP method, as in LB13), and an alternative approach (1SSP+[X/Fe]), where IMF and individual abundance ratios are fitted simultaneously.

- We find a very mild variation of Γ_b with [Mg/Fe] at fixed σ_0, implying that [Mg/Fe] plays a subdominant role in the variation of the IMF slope among ETGs.
- On the contrary, we find a strong, highly significant ($> 10\,\sigma$), correlation of the IMF slope with σ_0, regardless of the adopted methodology.

Since for a fixed IMF functional form (such as the bimodal distribution), Γ_b is proportional to the overall normalization (i.e. the mass-to-light ratio normalized to that for a Kroupa-like distribution), our results contrast with the claim of CvD12b, that the IMF should correlate more strongly with [Mg/Fe] than σ_0. We note that the models of CvD12b use [Fe/H] and not [Z/H] as an "overall" metallicity parameter. Therefore their [Mg/Fe] variations could be related to total metallicity. S14 found that for a sample of 34 ETGs in common between CvD12b and Atlas^{3D}, the dynamical constraints to the IMF appeared not to be consistent with the line strength analysis of CvD12b. Dynamical models correlate with velocity dispersion (σ_0) and not with [Mg/Fe]. Therefore, our results – based on spectral indices – are qualitatively more consistent with the results from dynamical modeling. In particular, the fact that Γ_b decreases slightly with [Mg/Fe], at fixed σ_0, when using the 1SSP+[X/Fe] fitting method, is similar to the results in S14 regarding the dynamical constraints (see fig. 4 of S14, and our Fig. 2). At the moment, the origin of the above discrepancies is not clear. As already noticed by S14, several possible effects might contribute, including (i) sample size/selection issues, as we analyze a sample of 126 stacked spectra, while CvD12b studied 38 (individual) galaxies; (ii) methodology, as we rely

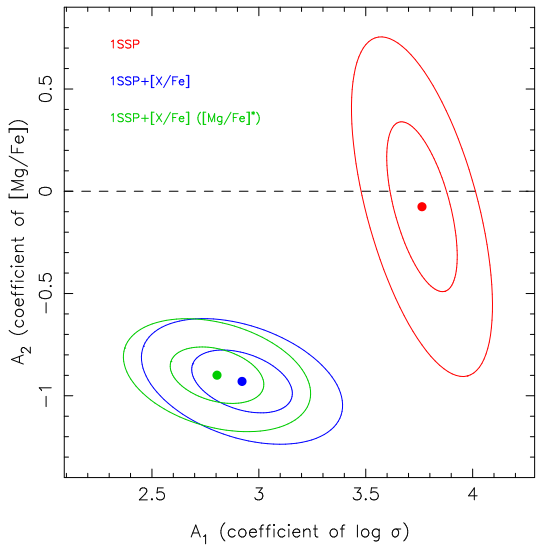

Figure 2. Best-fitting slopes of the bivariate correlation of Γ_b vs. $\log\sigma_0$ and [Mg/Fe] (Eq. 2). Different methods/samples are plotted with different colors, as labeled in the upper–right of the figure. Ellipses mark $1\,\sigma$ and $2\,\sigma$ normal confidence contours on the slope values. The horizontal dashed line represents a zero correlation with [Mg/Fe] at fixed σ_0. Notice that the $\log\sigma_0$ slope is highly significant in all cases, while the [Mg/Fe] slope depends on the adopted methodology, being fully consistent with zero when no abundance ratios are fitted to spectral indices (red dot and ellipses), or mildly *anticorrelated* if individual abundances are considered.

on line strengths, rather than spectral fitting, and adopt (MIUSCAT) stellar population models with varying total metallicity (in contrast to CvD12a models); (iii) systematics, on either stellar population models (for spectroscopic constraints) or the modeling of the (dark-)matter distribution in ETGs (for dynamical constraints); (iv) radial variations of the IMF, as the SDSS spectra cover $\sim 1R_{\rm eff}$ spatial scale, in contrast to the $R_{\rm eff}/8$ scale of CvD12b. The latter aspect is particularly relevant in light of our recent finding (MN15) that the IMF slope decreases with galacto-centric distance in massive ETGs (see also Pastorello et al. 2014), implying that local and global constraints to the IMF might result in different trends. We also remark that the present work does not imply that the central σ_0 (an integrated measurement) is the "causal" driver of the IMF in ETGs, but, rather, that [Mg/Fe] (possibly related to the timescale of star formation) is not driving the systematic variations of the IMF, at least over a $\sim 1R_{\rm eff}$ spatial scale. In particular, given the tight correlation between metallicity and σ_0 in ETGs, and the narrow dynamical range of metallicity in our stacked spectra at fixed σ_0 (LB13) , the values of Γ_b in Fig. 1 can also be considered to correlate with (total) metallicity. Hence, our integrated spectra cannot be used to infer the physical driver of the trend. Spatially resolved spectroscopic studies, extended to large samples of galaxies, with the aid of further advances in the modeling of stellar populations, should help in the future to address this issue (Martín-Navarro et al., in preparation).

ACKNOWLEDGMENTS

We thank Dr. M. Beasley, and the anonymous referee, for interesting comments and suggestions. We acknowledge the use of SDSS data (http://www.sdss.org/collaboration/credits.html), and support from grant AYA2013-48226-C3-1-P from the Spanish Ministry of Economy and Competitiveness (MINECO).

REFERENCES

Adelman-McCarthy, J. K., Agüeros, M. A., Allam, S. S., et al., 2008, ApJS, 175, 297
Auger, M. W., et al., 2010, ApJ, 724, 511
Cappellari, M., et al., 2012, Nature, 484, 485
Cappellari, M., et al., 2013, MNRAS, 432, 1862
Chabrier, G., PASP, 115, 763
Chabrier, G., Hennebelle, P., Charlot, S., 2014, ApJ, 796, 75
Cid Fernandes, R., Mateus, A., Sodré, L., Stasinska, G., Gomes, J. M., 2005, MNRAS, 358, 363
Cenarro, A. J., Gorgas, J., Vazdekis, A., Cardiel, N., Peletier, R. F., 2003, MNRAS, 339, L12
Conroy, C., van Dokkum, P., 2012a, ApJ, 747, 69 (CvD12a)
Conroy, C., van Dokkum, P., 2012b, ApJ, 760, 71 (CvD12b)
de La Rosa, I. G., La Barbera, F., Ferreras, I., de Carvalho, R. R., 2011, MNRAS, 418, L74
Dutton, A. A., Macciò, A. V., Mendel, J. T., Simard, L., 2013, MNRAS, 432, 2496
Ferreras, I., La Barbera, F., de la Rosa, I. G., Vazdekis, A., de Carvalho, R. R., Falcón-Barroso, J., Ricciardelli, E., 2013, MNRAS, 429, L15 (F13)
Ferreras, I., Weidner, C., Vazdekis, A., La Barbera, F., 2015, MNRAS Lett. in press (arXiv:1501.01636)
Hopkins, P. F., 2013, MNRAS, 433, 170
Johansson, J., Thomas, D., Maraston, C., 2012, MNRAS, 421, 1908
Kroupa P., Weidner C., Pflamm-Altenburg J., et al., 2013, *in Vol. 5: Galactic Structure and Stellar Populations*, ed. T. D. Oswalt & G. Gilmore (New York: Springer), 115
Kuntschner, H., et al., 2010, MNRAS, 408, 97
La Barbera, F., de Carvalho, R. R., de la Rosa, I. G., Lopes, P. A. A., Kohl-Moreira, J. L., Capelato, H. V., 2010a, MNRAS, 408, 1313 (Paper I)
La Barbera, F., et al., 2013, MNRAS, 433, 3017
McDermid, R. M., et al., 2014, ApJ, 792, 37
Martín-Navarro, I., La Barbera, F., Vazdekis, A., Falcón-Barroso, J., Ferreras, I., 2015, MNRAS, 447, 1037 (MN15)
Pastorello, V., et al., 2014, MNRAS, 442, 1003
Sansom, A. E., de Castro Milone, A., Vazdekis, A., Sánchez-Blázquez, P., 2013, MNRAS, 435, 952
Smith, R., Lucey, J. R., 2013, MNRAS, 434, 1964
Smith, R., MNRAS, 443, 69 (S14)
Spiniello, C., Trager, S., Koopmans, L. V. E., Conroy, C., 2014, MNRAS, 438, 1483 (STK14)
Spiniello, C., Trager, S., Koopmans, L. V. E., 2015, (arXiv:1401.1145)
Thomas, D., et al. 2005, ApJ, 621, 673
Thomas, D., Maraston, C., Johansson, J., 2011, MNRAS, 412, 2183
Tortora, C., Romanowsky, A. J., Napolitano, N. R., 2013, ApJ, 765, 8

van Dokkum, P. G., Conroy, C., 2010, Nature, 468, 940
Vazdekis, A., Casuso, E., Peletier, R. F., Beckman, J. E., 1996, ApJS, 106, 307
Vazdekis, A., Ricciardelli, E., Cenarro, A. J., Rivero-González, J. G., Díaz-Garcá, L. A., Falcón-Barroso, J., 2012, MNRAS, 424, 157 (MIUSCAT-I)